

ORIGINAL RESEARCH

OPEN ACCESS Check for updates



EphA2 and phosphoantigen-mediated selective killing of medulloblastoma by yδT cells preserves neuronal and stem cell integrity

Lola Boutin (Da, Mingzhi Liu (Da, Julie Déchanet Merville (Db, Oscar Bedoya-Reina (Dc, d, and Margareta T Wilhelm (Da

^aDepartment of Microbiology, Tumor and Cell Biology (MTC), Karolinska Institutet, Stockholm, Sweden; ^bCNRS, ImmunoConcept, UMR 5164, Bordeaux University, Bordeaux, France; School of Medical Sciences, Örebro University, Örebro, Sweden; Department of Women's and Children's Health, Karolinska Institutet, Stockholm, Sweden

ABSTRACT

Medulloblastoma (MB) is a pediatric brain tumor that develops in the cerebellum, representing one of the most common malignant brain cancers in children. Standard treatments include surgery, chemotherapy, and radiation, but despite a 5-y survival rate of approximately 70%, these therapies often lead to significant neurological damage in the developing brain. This underscores the urgent need for less toxic, more effective therapeutic alternatives. Recent advancements in cancer immunotherapy, including immune checkpoint inhibitors and CAR-T cell therapy, have revolutionized cancer treatment. One promising avenue is the use of Gamma Delta ($\gamma\delta$)T cells, a unique T cell population with potential advantages, such as non-alloreactivity, potent tumor cell lysis, and broad antigen recognition. However, their capacity to recognize and target MB cells remains underexplored. To investigate the therapeutic potential of $\gamma\delta T$ cells against MB, we analyzed the proportion and status of MB-infiltrated $\gamma\delta T$ cells within patient datasets. We next investigated the expression of $\gamma\delta T$ cell ligands on MB cells and identified the EphA2 receptor and the phosphoantigen/Butyrophilin complex as key ligands, activating Vγ9 Vδ1 and Vγ9 Vδ2 T cells, respectively, leading to significant MB cell lysis in both monolayer and spheroid models. Importantly, preliminary safety data showed that $y\delta T$ cells did not target differentiated neurons or neuroepithelial stem cells derived from induced pluripotent stem cells, underscoring the selectivity and safety of this approach. In conclusion, γδT cells trigger an efficient and specific killing of MB and would offer a promising novel therapeutic strategy.

ARTICLE HISTORY

Received 9 November 2024 Revised 24 March 2025 Accepted 24 March 2025

KEYWORDS

Gamma delta T cells; immunotherapy; medulloblastoma

Introduction

Medulloblastoma (MB), one of the most common malignant pediatric tumor of the central nervous system (CNS), accounting for 20% of all pediatric CNS tumors, represents a heterogeneous group of brain tumors usually found in the cerebellum. Current treatment protocols have improved the 5-y-overall survival (5y-OS) rate to 80% globally. Four main subgroups of MB have been identified by molecular classification: Wingless (WNT), Sonic Hedgehog (SHH), Group (Grp)3, and Group (Grp)4.² Prognosis is strongly linked to the MB subgroup, with WNT-activated MB having a more favorable outcome (90% 5y-OS) and Grp3, the less favorable (50% 5y-OS) with a high metastatic rate.³ MB patients are treated according to a standard of care, which includes surgical resection, adjuvant chemotherapy and, in some cases, craniospinal irradiation. However, this treatment often leads to systematic and irreversible neurological deficits, resulting in a decline in intellectual and cognitive function, due to damage of the healthy brain tissue.4 Highlighting the importance of identifying less toxic and more effective therapeutic alternatives for MB.

Recently, immunotherapy has paved the way to propose more specific and safer alternatives to conventional chemotherapies.

MB is known as a cold tumor with an immune evasive microenvironment, mostly limited to M2-like microglia and macrophage infiltration.⁵ In addition, MB is characterized by a low mutation burden and the absence of PD-L1 expression, which correlates with low T cell infiltration. While immune checkpointblockade (ICB) therapy (e.g. PD1/PD-L1, CTLA-4) has led to a major breakthrough for many solid tumors, MB does not seem to benefit from it.7 Adoptive cell therapies such as CAR-T or NK cell therapy are currently being evaluated in various clinical trials for pediatric brain tumors including MB patients, 8,9 with CAR-T cells targeting B7-H3, GD2, IL-13a, EphA2, or HER2 showing some promise.8 However, tumor cells can escape CAR-T cells by downregulating the expression of the target molecules, as has been demonstrated in 30-70% of patients undergoing therapy.10

γδT cells are an MHC-peptide unrestricted T cell population which recognizes conserved cellular stress patterns upregulated in infected and transformed cells. 11 They possess both adaptive and innate receptors such as a functional T cell receptor (TCR) associated with a CD3 molecule, as well as NKG2D and Toll-like receptors (TLR), which enable them to recognize a broad spectrum of ligands.¹² γδT cells express a TCR composed of Vγ and Vδ chains,

CONTACT Margareta T Wilhelm argareta.wilhelm@ki.se; Lola Boutin lola.boutin@ki.se Department of Microbiology, Tumor and Cell Biology (MTC), Karolinska Institutet, Biomedicum B7, Stockholm 17165, Sweden

Supplemental data for this article can be accessed online at https://doi.org/10.1080/2162402X.2025.2485535

the former defining the $\gamma\delta T$ subpopulation (V δ 1, V δ 2, and V δ 3), and the preferred location. Invariant V γ 9 V δ 2 T cells are the main population in the peripheral blood system, (>90% of the total $\gamma\delta T$) sensing phosphoantigens (pAgs) level dysregulation in transformed or infected cells, whereas Vδ1 and Vδ3 subpopulations are mainly present in tissues where they are involved in immune surveillance but also in the maintenance of tissue homeostasis.¹³

Allogeneic therapies based on $\gamma \delta T$ cells have been shown to be clinically safe and effective in various cancers, demonstrating the potential of using an allogeneic γδT cell bank for tumor immunotherapy. ^{14–16} However, the ability of $\gamma \delta T$ cells to target and eliminate MB cells is poorly documented. Here, we show that both Vγ9Vδ2T and Vγ9Vδ1T cells can specifically eliminate MB cells without affecting healthy neural stem cells or neurons, highlighting the potential of using $\gamma \delta T$ cells for immunotherapy of medulloblastoma and other pediatric CNS

Materials and methods

Deconvolution of bulk MB tumor samples and TIL

Bulk RNA sequencing datasets were downloaded from GEO portal: Normal cerebellum (GSE44971) and MB patients (GSE37418 and GSE85217). Assessments of leucocyte fractions from the specified transcriptomes were performed by applying CIBERSORT (https://cibersort.stanford.edu/) with the matrix LM-7 as previously described. 17,18 Abundances were calculated from the CIBERSORT results and Sample Enrichment Score (SES). SES was computed by applying the open-source software AutoCompare-SES (https://sites.goo gle.com/site/fredsoftwares/products/autocompare_ses) with normalized settings. Then, the open-source software DeepTIL (https://sites.google.com/site/fredsoftwares/pro ducts/deeptil) was used to automatically compute the abundance of the seven leucocyte subsets.

TCR repertoire analysis

To conduct the TCR repertoire analysis, we used the Riemondy et al. MB immune cell landscape dataset obtained by using single-cell sequencing.⁶ Briefly, 29 samples were single-cell sequenced using 10X Genomics to a depth of 50,000 reads per cells, and processed using CellRanger and Seurat. The resulting dataset contains normalized expression for 4,669 MN tumor-infiltrating immune cells including clusters of microglia, myeloid, neutrophil, NK, T, and B cells. This data was downloaded from the pediatric Neurooncology Cell Atlas (pneuroonccellatlas.org) available at https://github.com/rnabioco/medulloblast on 08/09/2023. The available metadata from Supplementary Table 1 of Riemondy et al. was included in the analysis. To study the γδ repertoires in T cells of MB, BAM files from single-cell alignments of the 29 samples analyzed were obtained from the GEO SuperSeries accession number GSE156053 on 09/ 12/2023. These files were further processed with TRUST4, to

determine the repertoires for each cell independently, following their barcodes. 19

T cell differentiation state analysis

To determine the differentiation state of T cells, gene signatures for 1) naïve, 2) resident, 3) pre-exhausted, 4) exhausted, and 5) effector-memory cells were generated (Table S1). For each of these gene lists a signature score was computed as the average expression of each reference gene sets, minus the average of a (n) randomly selected set of genes (where n =max [# reference genes, 50]). The signature score provides an estimation of the transcriptional resemblance of each cell to each reference cluster of interest. Additionally, the normalized expression for each gene within these signatures was obtained.

Analysis of ligand expression and $\gamma \delta T$ cell activation

Cell culture conditions and ex-vivo yδT cell expansion are described in detail in supplemental material and methods (Sup. Mat&Met). Primary γδT cells were isolated from anonymized buffy coat from healthy donors obtained from the department of Klinisk Immunologi och transfusionsmedicin at Karolinska University Hospital. Local regulations state that working with blood from anonymous healthy human donors requires no ethical permit. For CD107a surface mobilization assays, target cells were treated for 18 h with zoledronic acid (Sigma, SML0223) in their maintenance media. 1×10^5 target cells were co-cultured for 4 h with amplified yδT cells (E/T ratio 1:1) in RPMI-1640 supplemented with 10% FBS containing Golgi Stop (BD Biosciences 554724) and anti-CD107a mAb for 4 h. Cells were harvested and stained with anti-pan γδ TCR, anti-Vδ2, and anti-Vδ1 mAbs. For CD69 expression, target cells were co-cultured with JRT3-MAU cells (E/T ratio 1:1) in RPMI-1640 supplemented with 10% FBS for 4 h. Cells were harvested and stained with anti-Vδ1 and anti-CD69 mAbs. Flow cytometry data were acquired using BDCanto II cytometer (BD Biosciences) and analyzed using FlowJo v.10 software (Treestar). All antibodies used for flow cytometry assays are described in supplemental materials (Sup. Mat&Met).

LDH-release cytotoxicity assay

For monolayer killing assay, targets cells were seeded in flatbottom 96-well plates in their maintenance media 1-d prior to co-culture. For spheroid killing assay, 15×10^3 target cells were seeded in U-bottom 96-well low adherence plates (BRANDplates®, inertGrade™) 4 d prior co-culture in NES media. Target cells were treated for 18 h with zoledronic acid (Sigma, SML0223), followed by co-culture with amplified γδT cells (E/T ratio 10:1) in RPMI-1640 supplemented with 5% Human serum (Sigma, H5667) for 8 h. Supernatants were collected and used for LDH (lactate dehydrogenase) measurement using CytoTox 96° kit (Promega, G1780) according to the manufacturer's protocol, and quantified by FLUOstar Omega plate reader (Absorbance 490 nm, BMG LABTECH). The percentage of target cell lysis was calculated as follows: ((experimental release - spontaneous release)/(maximum release spontaneous release)) × 100. Spontaneous and maximum release values were determined by adding either medium or lysis buffer (provided in the kit) to target cells without T cells. For NKG2D blocking assay, 10 $\mu g/mL$ of anti-NKG2D mAb was added to the $\gamma\delta$ T cells 20-min prior co-coculture and kept throughout the experiment.

Results

$\gamma \delta T$ cells are predicted to be present in healthy cerebellum and in MB patients

The presence of $\gamma\delta T$ cells in healthy CNS and in CNS tumors has been poorly reported. Moreover, the difficulty of transcriptionally separating $\gamma\delta T$ from CD8⁺ $\alpha\beta T$ and NK cells makes it difficult to predict their proportion from tissue or tumor

mRNA samples.²⁰ Recently, an updated version of an immunosignature (LM-7) CIBERSORT deconvolution matrix optimized for $\gamma\delta T$ cells was developed.¹⁷ Using the LM-7 matrix, we estimated the immune infiltration by comparing healthy cerebellum from five fetal and four adult tissues (GSE44971) with 76 MB patients (GSE37418). As previously described, we found that the immune landscape of MB is not different from that of non-tumoral tissue (Figure 1a, Table S2).²¹ In particular, we found no significant differences in the proportion of different immune cell populations between fetal/adult cerebellum and MB (two-side Kruskal–Wallis, p > 0.05) for the predictions of CIBERSORT and SES+CIBERSORT, with the sole exception of CD4⁺ T cells that present a marginal significant difference between fetal and malignant tissues (two-side Mann-Whitney U, p = 0.013) for the CIBERSORT prediction

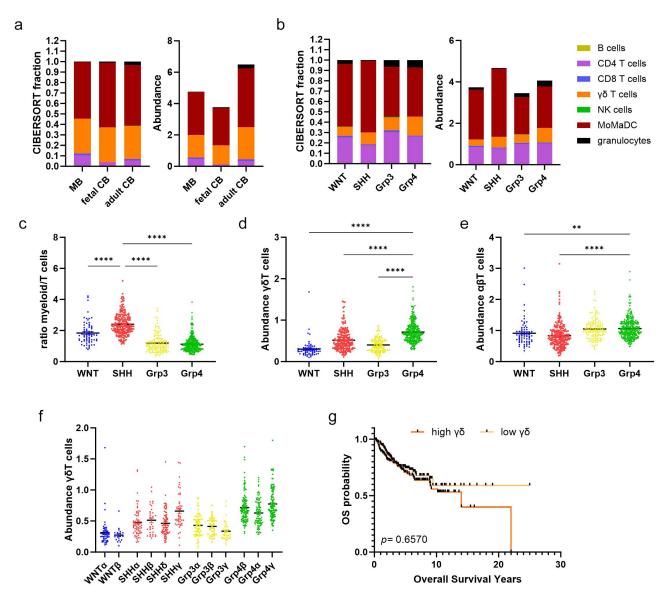


Figure 1. γδT cells abundance in MB tumors. (a) Immune cell infiltration and abundance in MB (n=76) versus normal fetal (n=5) and adult (n=4) cerebellum (CB) samples. (b) Immune cell infiltration and abundance in MB subgroups (WNT-MB n=70; SHH-MB n=222; Grp3-MB n=143; Grp4-MB n=325). (c) Ratio of myeloid cells/T cells (CD4+CD8+ γδT cells) in SHH-MB versus other subgroups. Statistical analysis was performed using two-way ANOVA followed by Dunnett test to correct WNT-MB, Grp3-MB and Grp4-MB vs SHH-MB (***p = 0.0001). (d) γδT and (e) αβT cells abundance across MB subgroups. Statistical analysis was performed using one-way ANOVA followed by Dunnett tests to correct for WNT-MB, SHH-MB, and Grp3-MB vs Grp4-MB (**p = 0.0037; ***p < 0.0001). (f) γδT abundance across MB subtypes. (g) Overall survival of patients grouped according to high or low abundance of γδT cells in MB all subgroups (1st and last quartile, n = 306 per group). Significance was determined by log-rank test – nonsignificant differences are not displayed in the figure.

(Figure S1a). The abundance value was similar to previous reports in which MB had the lowest immune cell abundance of all tumors, including other brain tumors, making it one of the most immune-evasive tumors. 17

To further analyze the differences in immune cell infiltration, and specifically $\gamma \delta T$ cell infiltration between the different MB subgroups, we used a larger MB patient cohort (GSE85217, 763 patients). We observed some differences in immune cell infiltration between the subgroups (Figure 1b, Table S3). SHH-MB has an increased fraction of myeloid cells and a lower proportion of granulocytes compared to other subgroups, consistent with previous findings (Figure S1b,c).²² The ratio of myeloid cells to T cells is also significantly higher in SHH-MB (Figure 1c). CD4⁺ T cells are the major lymphoid subsets in MB, followed by $\gamma \delta T$ cells (Figure 1b, Table S3). In contrast, CD8⁺T cells and NK cells, two cytotoxic subsets, are found in very low abundance in the tumor (Figure 1b, Table S3). Additionally, Grp3-MB shows the highest NK cells abundance, while B cells remain in very low abundance to undetected for all subgroups (Figure S1d,e).

Interestingly, the frequency of $\gamma\delta T$ cells in MB differs between the subgroups, with the highest score in Grp4-MB, while αβT cells (CD8⁺ and CD4⁺) are more homogeneously distributed in the subgroups (Figure 1d,e). In addition, the four MB subgroups can be further divided into 12 subtypes according to age, histology, methylation profile, and driver mutations,³ and the abundance score of γδT cells varies between subtypes in the same subgroup, except for WNT-MB (Figure 1f). We observed an increase of $\gamma\delta T$ cell score in SHH γ and Grp4y and a slight decrease in Grp3y subtypes (Figure 1f). $y\delta T$ cell infiltration in many tumor types has been shown to be associated with a favorable outcome. 23,24 We investigated whether the $\gamma \delta T$ cell scores correlate with prognosis in MB. Using the same cohort, patients were divided into $\gamma \delta T$ cell high vs $\gamma \delta T$ cell low abundance score (1st vs 4th quartile), but we found no significant correlation between γδT cell frequency and survival (p = 0.6570, log-rank test, Figure 1g). In conclusion, we show here that $\gamma \delta T$ cell infiltration is predicted for normal cerebellum and MB, with some differences between the different MB subgroups and subtypes, but γδT cell frequency did not correlate with prognosis, possibly due to its global low frequency.

Tumor infiltrated $\gamma \delta T$ cells show a tissue resident phenotype

To further characterize the phenotype and activation state of γδT cells in MB, we extracted the BCR/TCR repertoire using the Trust4 algorithm from a single-cell RNA dataset of 28 MB patients (GSE155446, 1 WNT, 9 SHH, 7 Grp3, and 11 Grp4). 19 Unfortunately, the number of B and T cells recovered by the algorithm was low compared to the clustering shown in the pediatric neuro-oncologic cell atlas.⁶ In total, 21 B cells, 56 αβT cells, and 52 γδT cells were identified by the algorithm with a complete or partial BCR/TCR identification (Table S4). Interestingly, the γ - and β -VJC segments were recovered better than their δ - and α - pairs. Therefore, we focused our analysis of $\gamma \delta T$ -infiltrated cells on the γ -chain. Analysis of the variable (V) y-segment repertoire revealed a high diversity with

a dominance for recombination of TRGV2, TRGV9, and TRGV10 genes in all MB subgroups (Figure 2a). TRGV10 is characterized as a pseudogene (Vy type III) and results in a nonfunctional γδTCR.²⁵ In addition, TRGV2, TRGV4, and TRGV8, already identified as brain-specific γδTCR signatures,²⁶ were present in MB (Figure 2a). Interestingly, the public TRGV9 clonotype (CALWEVQELGKKIKVF), which is present in the blood from fetal to adult life,²⁷ was detected in one MB patient (Table S4). We next compared the diversity of the TRGV and TRGJ repertoires in the different MB subgroups (Figure 2b). Grp3-infiltrated γδT cells showed a significant reduction in TRGV and TRGJ diversity compared to the SHH- and Grp4-MB and had the highest proportion of nonfunctional TRGV10⁺ cells (Figure 2b). However, the CDR3 length distribution of Grp3-infiltrated γδT cells is greater than that in the other subgroups ($\Delta 9$ vs $\Delta 6$ or $\Delta 7$ amino acids for SHH- and Grp4-MB, respectively) (Figure 2c). Overall, the analysis of the γδTCR repertoire revealed no specific clonal expansion, suggesting a lack of tumor-specific reactivity.

To confirm this hypothesis, we examined the differentiation status of $\gamma \delta T$ and $\alpha \beta T$ cells identified by the Trust4 algorithm, independent of the MB subgroup. We compared gene expressions specific to naïve, effector memory, resident memory, preexhausted, and exhausted T cells (Table S4). There were few differences between infiltrated γδT and αβT cells, which preferentially expressed ILR7, CCL5, GZMK, GZMA, and CD69 (Figure 2d). Evaluation of T cell differentiation state gene signatures of the T cell differentiation state revealed a phenotype enriched with resident memory cells that neither proliferate (KI67^{low}), show proinflammatory activity (IFNG^{low}), nor exhibit chronic activation-induced exhaustion (PDCD1^{low}, HAVCR2^{low}) (Figure 2e).

In summary, endogenous γδ T-infiltrated cells in MB do not express markers that would suggest active involvement in antitumor immunity in MB.

MB cells express γδΤ activating receptor ligands

Our analysis suggests that γδT cells infiltrate MB tumors but are insufficient in number and not functionally active. However, one of the main advantages of $\gamma \delta T$ cells is that they allow for ex-vivo expanded allogeneic immunotherapy due to their HLA-unrestricted activation. Therefore, we investigated which known ligands of human γδTCRs or co-receptors are expressed by MB cells to identify a γδT cell subset that could target MB cells. We examined a panel of seven MB cell lines, which are considered relevant in vitro models, covering three of the four MB subgroups (excluding WNT).²⁸ This included two paired primary (P) and recurrent (R) tumors for Grp3 and Grp4-MB. We stained for γδTCR ligands: CD1d, CD1c, Ephrin Type-A receptor 2 (EphA2), and Annexin A2 (ANXA2); NKG2D ligands: UL16 binding protein (ULBP)2/5/6; MHC class I chain-related protein (MIC)A/B; and DNAM-1 (CD226) ligands: CD112 and CD155 (Figure 3, Figure S2). Flow cytometry results showed that all MB cell lines were negative for CD1c and that only DAOY cells presented weak expression of CD1d (Figure 3, Figure S2), as previously reported.²⁹ Overall, lipid presentation by CD1 molecules does not appear to be a promising target candidate for MB.

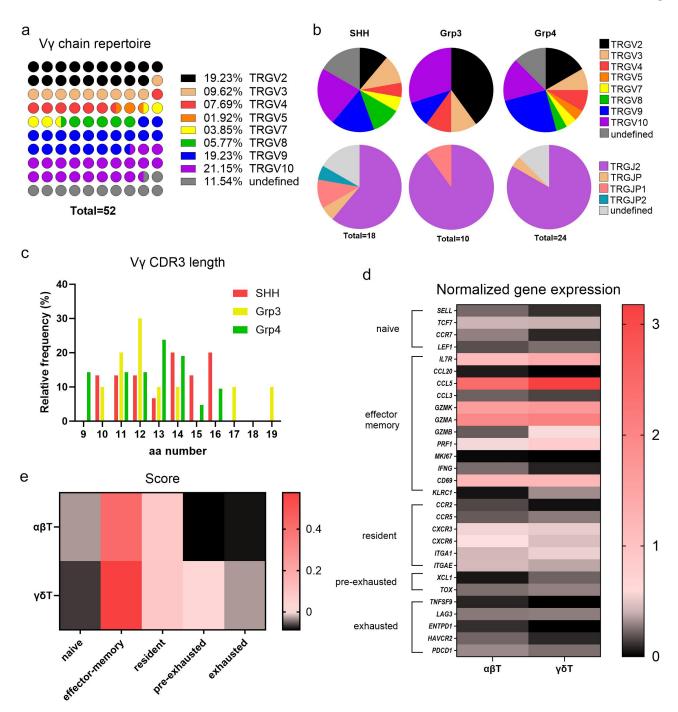


Figure 2. Infiltrated γδTCR repertoire and differentiation state (a) TCR *TRGV* gene repertoire repartition (n = 52 γδT cells, in 24 patients, GSE156053). (b) *TRGV* and *TRGJ* gene expression repartition across MB subgroups. (c) Relative frequency of the Vγ chain CDR3 across MB subgroups. (d) Normalization of 30 gene expressions of the identified αβT and γδT cells representative of five T cell differentiation state (n = 56 αβT cells and n = 52 γδT cells). (e) Signature score of each T cell differentiation state cluster.

However, all MB cell lines express EphA2 and ANXA2 (Figure 3, Figure S2), specific ligands for Vγ9Vδ1 and Vγ8Vδ3T cells, respectively. CD112 and CD155, ligands of DNAM-1 an adhesion molecule, are also expressed by all MB cell lines tested (Figure 3, Figure S2). Binding of DNAM-1 promotes activation of T/NK cells and cytolytic degranulation. However, CD112 and CD155 are also ligands for the checkpoint inhibitor TIGIT, which

could promote immunosuppression. Interestingly, only the SHH-MB cell lines (DAOY, UW228–3, and ONS-76) were found to express NKG2D ligands (Figure 3, Figure S2). D425 and CHLA-01-MED cells show a very low expression of ULBP2/5/6, but no expression of MICA/B (Figure 3, Figure S2). Their respective relapses, D458 and CHLA-01 R-MED, are found negative for both (Figure 3, Figure S2), suggesting that the immunogenicity of Grp3 and Grp4-MB

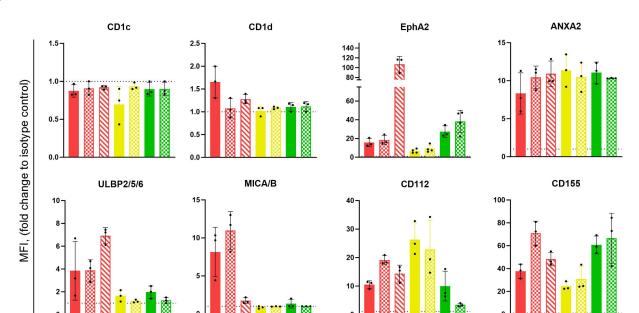


Figure 3. γδTCR, and γδT co-receptor ligand expression by MB cell lines. Fold change of MFI (Median of fluorescence) of expression of γδTCR, and γδT co-receptor ligands on seven MB cell lines compared to corresponding isotype controls, acquired by flow cytometry; n = 3-4 independent experiments (dashed line = 1, threshold of expression).

Grp3 D425(P) D458(R)

for the activation of NK and $\gamma\delta T$ cells may be reduced. In summary, we identified a $\gamma\delta T$ cell ligand signature in MB cells that is subgroup-dependent, guiding to which $\gamma\delta T$ cell subset that can target MB cells.

SHH DAOY UW228-3 ONS-76

EphA2-expressing MB cells trigger Vγ9 Vδ1 T cell activation

EphA2 is a member of the Ephrin receptors, the largest receptor tyrosine kinase receptor family, and is involved in several biological processes such as neuronal development, cytoskeleton dynamic, migration, cell proliferation, and angiogenesis. It is found to be overexpressed in tumors compared to normal tissues, making it a good target for cancer therapy,³³ which is supported by the development of CAR-T cells targeting EphA2 for Grp3-MB and ependymoma.³⁴ As proof-of-principal for EphA2 as a target ligand for $V\gamma9V\delta1T$ cells in MB, we used the Jurkat lymphoblastic cell-line JRT3 (β-TCR chain defective), engineered to express the Vγ9Vδ1-MAU TCR that was previously shown to recognize EphA2.30 The JRT3 model lacks cytotoxic capabilities, but can be used to assess $V\gamma9V\delta1T$ cell activation. We co-cultured JRT3-MAU with MB cell lines or with healthy iPSC-derived neuroepithelial stem (NES) cells and measured the expression of the activation marker CD69 on JRT3-MAU by flow cytometry. Co-culture with MB cell lines induced expression of CD69, regardless of MB subgroup, resulting in strong activation of JRT3-MAU cells, except for the relapse cell-line CHLA-01 R-MED, which showed a lower response (Figure 4a). However, co-culture with non-cancerous healthy NES cells resulted in significantly less activation of JRT3-MAU (Figure 4a). Interestingly, the expression level of EphA2 does not seem to correlate with the activation potential. To confirm this observation, we measured EphA2 expression in NES cells, which was in the same range as in the D425 cell

line but activated JRT3-MAU to a much lower extent (Figures 3, 4b). These results suggest the presence of accessory signals in tumor cells that potentiate JRT3-MAU activation in addition to EphA2.

Grp4 CHLA-01-MED(P) CHLA-01R-MED(R)

Next, we examined EphA2 expression in both healthy cerebellum and MB patients using a publicly available dataset and found that the *EPHA2* gene expression is significantly upregulated in Grp3-MB and WNT subgroups compared to normal cerebellum (Figure 4c). To demonstrate the potential of V γ 9V δ 1T cells targeting Grp3-MB, we co-cultured JRT3-MAU with the Grp3-MB PDX MB-LU-181, using D425 cells as a reference. Results showed that JRT3-MAU upregulate CD69 expression in the presence of Grp3-MB PDX, yet to a lesser extent than with the D425 cell line (Figure 4d). Overall, these results confirmed the potential of targeting EphA2-positive MB cells with V γ 9V δ 1T cells in a tumor-specific manner.

Amino bisphosphonates sensitize MB cells, but not healthy neuronal cells to Vy9 Vδ2T lysis

Cancer cells have a dysregulated metabolism with increased protein and lipid synthesis. Cholesterol, an essential component of the cell membrane, is produced via the mevalonate synthesis pathway. One of the intermediates of this pathway, isopentenyl pyrophosphate (IPP), can bind to the intracellular domain of a member of the butyrophilin family, BTN3A1, and trigger the activation of V $\gamma 9V\delta 2T$ cells. 36,37 Aminobisphosphonate (NBP) molecules such as Zoledronate (zol) can increase intracellular IPP levels by inhibiting the farnesyl diphosphate synthase in target cells, which then enhance V $\gamma 9V\delta 2T$ cell activation (Figure 5a).

BTN3A1 and its partner, BTN2A1, are expressed in majority of human healthy and tumoral tissues. 38,39,40 We tested whether V γ 9 V δ 2T cells can naturally recognize MB cells or

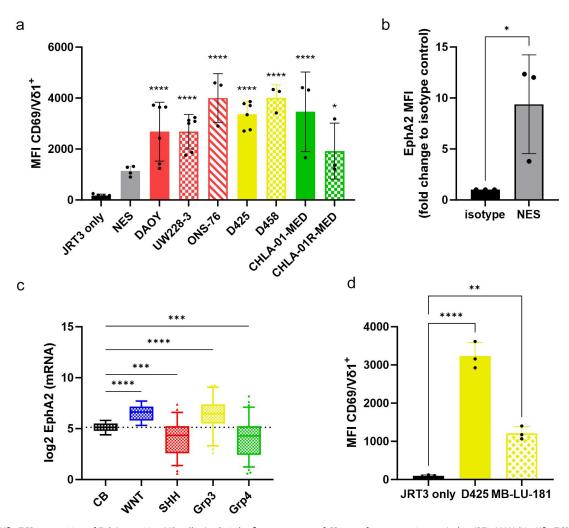


Figure 4. Vy9 V δ 1 TCR recognition of EphA2-positive MB cells. Analysis by flow cytometry of CD69 surface expression on Jurkat JRT3 MAU (Vy9V δ 1 TCR positive) after a 4 h-co-culture (E/T ratio 1:1) with (a) neuroepithelial stem cells (NES) and MB cell lines, n=3-5, or (d) Grp3 PDX cells. n=3 independent experiments. Statistical analysis was performed using one-way ANOVA followed by Dunnett tests to correct for multiplicity (*p<0.05; ****p=0.0001; *****p<0.0001). (b) Fold change of MFI (Median of fluorescence) of EphA2 expression on NES. n=3 independent experiments. Statistical analysis was performed using unpaired t-test (*p<0.05). (c) EPHA2 mRNA expression in human MB subgroups versus normal human cerebellum (CB) (WNT-MB n=17; SHH-MB n=59; Grp3-MB n=56; Grp4-MB n=91; CB n=9). Statistical analysis was performed using Brown-Forsythe and Welch's ANOVA test followed by Dunnett tests to correct for multiplicity (***p<0.0005; *****p<0.0001) – nonsignificant differences are not displayed in the figure.

be sensitized by zol treatment. NES and MB cells were treated overnight with 0, 1, or 10 μM of zol followed by co-culture with ex-vivo expanded peripheral γδT cells isolated from healthy donors, the majority of which consisted of $V\delta 2^+ \gamma \delta T$ cells (Figure 5b). The expression of the degranulation marker CD107a was analyzed on $V\delta2^+$ $\gamma\delta T$ cells by flow cytometry. As expected, untreated NES and MB cells did not trigger Vγ9Vδ2T cell degranulation (Figure 5c). However, MB cells treated with 10µM zol, but not zol-treated NES cells, were able to significantly activate Vγ9Vδ2T cells (Figure 5c). The suboptimal dose of 1 µM showed a difference in the sensitivity of each cell line to zol-treatment, with SHH cell lines and D425 cells inducing CD107a expression on Vγ9Vδ2T cells, but not D458 and Grp4-MB cells. Furthermore, we detected differences between donors in terms of zol-mediated activation against MB (Figure 5c).

Next, we investigated whether zol treatment was sufficient to induce killing of MB cells by V γ 9V δ 2T cells. We cultured MB cells, either as adherent monolayer (m) or as spheroids (sph), together with ex vivo expanded $\gamma\delta$ T cells

and quantified LDH release as a measure of cell death. LDH release results showed that SHH-MB treated with zol induced killing by γδT cells in both monolayer and spheroid conditions (Figure 5d). The cytotoxic potential of γδT cells against zol-treated SHH-MB cells is donorand target-dependent. Interestingly, the UW228-3 and ONS-76 cell lines are eliminated more efficiently in spheroid form. We hypothesized that the percentage of killing in monolayer could be underestimated by the readout method, as brightfield images taken after co-culture showed no remaining adherent MB cells (figure S3). Considering that we found that SHH-MB cells express NKG2D ligands, we further hypothesized that NKG2D might act in synergy with TCR activation against SHH-MB. However, NKG2D blocking on γδT cell did not affect the killing potential of zol-treated SHH-MB cells (Figures 5e, S3). The CD107a results indicated that Grp3- and Grp4-MB were less sensitive to zol treatment, so the zol concentration was increased to 50 µM. Since Grp3- and Grp4-MB are naturally suspension cell types, the treatment and co-culture

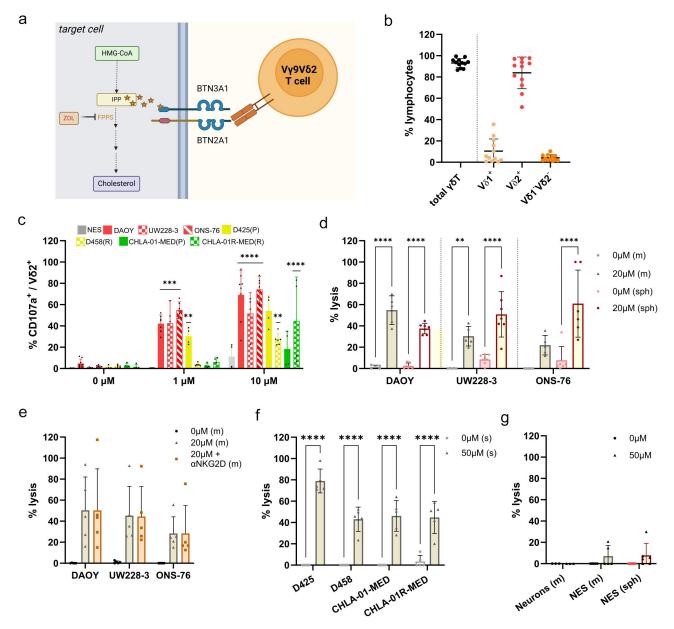


Figure 5. Vγ9Vδ2 TCR recognition of zoledronate-treated MB cells. (a) Schematic of the action of zoledronate in the cholesterol synthesis pathway leading to the activation of the Vγ9Vδ2 TCR via the BTN3A1/2A1 complex. (b) Percentage of total γδT cells in the ex vivo expanded population and percentage of the different γδT cell subsets assessed by flow cytometry. n = 12 donors (c) analysis by flow cytometry of CD107a expression on ex vivo-expanded human Vδ2T cells after 4 h of co-culture neuroepithelial stem cells (NES) and MB cell lines treated with 0 or 10 μm of zol (E/T ratio 1:1). n = 4-6 donors. (d)-(g) Analysis of cytotoxicity by LDH release in the supernatant, after 8 h-co-culture with ex vivo expanded γδT cells, by (d) SHH-MB cell lines grown in monolayer (m) or spheroid (sph), treated with 0 or 20 μm of zol. n = 5-7 donors; (e) by SHH-MB cell lines grown in monolayer (m), treated with 0 or 20 μm of zol with or without pre-conditioning with NKG2D blocking antibody (10 μg/ml) n = 5 donors; (f) by Grp3- and Grp4-MB grown in suspension (s), treated with 0 or 50 μm of zol. n = 5 donors; (s) by differentiated neurons and NES grown monolayer (m) or spheroid (sph), treated with 0 or 50 μm of zol. n = 3-6 donors; statistical analysis was performed using two-way ANOVA followed by (c) Dunnett, (d) Tukey (e)- (g) Sidak tests to correct for multiplicity (*p < 0.05; **p = 0.000; ***p = 0.000; ****p = 0.000; ****p = 0.000; *****p = 0.000; ****p = 0.000; ***p = 0.000; ***p = 0.000; ***p = 0.000; ***p

were performed accordingly. Zol-treated D425 reached an average of 80% of lysis, while the other three cell lines are closer to 45% (Figure 5f). The Grp4-MB cell lines CHLA-01 and CHLA-01 R grow as large neurospheres and have a lower proliferation rate than the Grp3 cells, which could explain the difference. However, the difference between the D425 and D458 cell lines could be the result of resistance acquired at relapse.

Finally, we examined the off-target effect of zol treatment on both proliferating NES cells and post-mitotic neurons. We treated the neuronal cells both as monolayer and as spheroids with high doses of zol (50 μ M). The co-

culture of zol-treated NES cells and neurons did not induce significant cytotoxicity-mediated by $V\gamma9V\delta2T$ cells, demonstrating that zol treatment triggers specific targeting and killing of MB cells by $V\gamma9V\delta2T$ cells while sparing healthy stem and differentiated neuronal cells (Figure 5g).

Discussion

CNS tumors remain among the most challenging to cure due to the complexity of the surrounding environment. Brain cells are very sensitive to conventional cancer therapies such as

chemotherapies and radiotherapies, 41 which have a significant impact on treatment outcomes and the long-term quality of life of survivors. Given that MB develops in the cerebellum, which controls physical movements, balance, and coordination, 42 it is crucial to develop less toxic therapies to preserve these important bodily functions.

A healthy immune system can distinguish between normal cells and infected or transformed cells. In cancer patients, however, the immune system is often impaired. Nonalloreactive and highly cytotoxic, γδT cells are a promising approach for allogeneic cell therapy in cancer patients. 43 Here, we demonstrate that MB patients may benefit from allogeneic γδT cell transfer. We confirm previous studies that the MB microenvironment lacks sufficient functional cytotoxic T cells, including both $\alpha\beta T$ and $\gamma\delta T$ cells, to elicit a sufficient anti-tumor response from the autologous T cells. The small numbers of $\alpha\beta T$ and $\gamma\delta T$ cells identified by the TCR repertoire algorithm Trust4 showed no significant clonal expansion or expression of activation/exhaustion markers, suggesting that conventional ICB therapy may show limited efficacy in MB patients. 44 However, the low TCR recovery – potentially due to insufficient sequencing quality or depth - necessitates a cautious interpretation of the conclusion. Future sequencing experiments with fresh patient samples and protocols optimized for TCR chain repertoire analysis could provide better insights.

We showed that MB cells express several ligands recognized by different γδTCR receptors and co-receptors (NKG2D and DNAM1), indicating the potential to target them with the corresponding γδT cell subset. We tested the activation potential of different γδT cell subsets against MB cell lines based on the TCR ligands they expressed. First, we demonstrated that seven MB cell lines and one PDX expressed EphA2 and activated Vγ9Vδ1-MAU TCR Jurkat cells. Similarly, CAR-T cells targeting EphA2 have shown strong anti-tumor potential in an in vivo Grp3-PDX model.34 However, these CAR-T cells lack the multipotency of multiple activating receptors expressed by γδT cells, which is an advantage in heterogeneous solid tumors. On the other hand, maintaining and expanding T cell clones in culture is challenging, so using the natural MAU clone may not be a viable therapeutic option. An alternative is TCRengineered T cell therapy, where the Vγ9Vδ1 TCR may be integrated into adoptive cell therapy (ACT) candidates, such as γδT or NKT cells. The latter are particularly interesting as they retain their endogenous TCR and can present dual-TCR recognition. 45 Additionally, the zol treatment can sensitize MB cells to killing by ex vivo expanded Vγ9Vδ2T cells. Zol, commercially available as Zometa®, is prescribed for bone diseases, including bone malignancies and osteoporosis. We demonstrated the direct anti-tumor potential of zol against MB cells; however, it has also been reported that zol can inhibit protumoral macrophages and microglia in a breast cancer brain metastasis model.⁴⁶ Importantly, both Vγ9Vδ1 and Vγ9Vδ2 T cell activation and killing were restricted to tumor cells, as normal NES and differentiated neurons did not triggering γδT cell activation, demonstrating the specificity of tumor cell targeting.

T cell-based therapies, including CAR-T cells and T cell engagers (TCE), face safety concerns, particularly regarding immune effector cell-associated neurotoxicity syndrome (ICANS) and cytokine storm syndrome (CSS).⁴⁷ However, the first clinical trial of allogeneic intravenous Vγ9Vδ2 T cell transfer for solid tumors did not report severe side effects associated with the ACT. 14 Nevertheless, there is currently no clinical data on the safety of intraventricular infusion of allogeneic γδT cells in patients, making it essential to identify potential side effects associated with this therapeutic strategy. A phase II clinical study using autologous Vγ9Vδ2 T cells genetically modified to resist Temozolomide, a conventional chemotherapy used for glioblastoma, is ongoing and could provide future indications regarding the safety of intracranial injection of $\gamma \delta T$ cells (NCT05664243).

In conclusion, our study is the first to support the therapeutic potential of allogeneic γδT cells for MB patients and their potential as a safer alternative to conventional treatment.

Acknowledgments

The authors thank the Biomedicum Flow Cytometry facility (BFC) for technical assistance. Part of the computations and data handling were enabled by resources provided by the National Academic Infrastructure for Supercomputing in Sweden (NAISS), partially funded by the Swedish Research Council through grant agreement no. 2022-06725. We thank everyone in the Wilhelm lab for technical assistance and helpful discussions.

Disclosure statement

No potential conflict of interest was reported by the author(s).

Funding

Cancerfonden [22 2236 Pj], Barncancerfonden [PR2021-0080], Radiumhemmets Forskningsfonder [#214173], and Vetenskapsrådet [2020-1427, 2023-02206]. Swedish Childhood Cancer Foundation grants TJ2021-0137 and [PR2021-0129] (O.C.B-R), KI Forskningsbidrag grant [2022-01925] (O.C.B-R).

ORCID

Lola Boutin (b) http://orcid.org/0000-0001-7928-6731 Mingzhi Liu http://orcid.org/0000-0001-5842-8307 Julie Déchanet Merville http://orcid.org/0000-0001-7521-9531 Oscar Bedoya-Reina (D) http://orcid.org/0009-0001-1703-2258 Margareta T Wilhelm http://orcid.org/0000-0002-0516-9724

Author contributions

Conception and design of the study: L.B and M.W.; Analysis and interpretation of the data: L.B. Generation and acquisition of data: L.B, M.L, O. B-R. Contribution of new reagents: J.D.M. Statistical analysis: L.B and O. B-R. Writing original draft of manuscript: L.B, O.B-R., J.D.M., and M.W. All authors have reviewed, read, and approved the submitted version of the manuscript.

Data availability statement

All data relevant to the study are included in the article or uploaded as supplementary information



References

- 1. Packer RJ, Gajjar A, Vezina G, Rorke-Adams L, Burger PC, Robertson PL, Bayer L, LaFond D, Donahue BR, Marymont MH, Muraszko K. Phase III study of craniospinal radiation therapy followed by adjuvant chemotherapy for newly diagnosed average-risk medulloblastoma. JCO. 2006;24:4202-4208.
- 2. Taylor MD, Northcott PA, Korshunov A, Remke M, Cho Y-J, Clifford SC, Eberhart CG, Parsons DW, Rutkowski S, Gajjar A, et al. Molecular subgroups of medulloblastoma: the current consensus. Acta Neuropathol. 2012;123(4):465-472. doi: 10.1007/ s00401-011-0922-z.
- 3. Cavalli FMG, Remke M, Rampasek L, Peacock J, Shih DJH, Luu B, Garzia L, Torchia J, Nor C, Morrissy AS, et al. Intertumoral heterogeneity within medulloblastoma subgroups. Cancer Cell. 2017;31(6):737-754.e6. doi: 10.1016/j.ccell.2017.05.005.
- 4. Mulhern RK, Palmer SL, Merchant TE, Wallace D, Kocak M, Brouwers P, Krull K, Chintagumpala M, Stargatt R, Ashley DM, et al. Neurocognitive consequences of risk-adapted therapy for childhood medulloblastoma. JCO. 2005;23(24):5511-5519. doi: 10.1200/JCO.2005.00.703.
- 5. Diao S, Gu C, Zhang H, Yu C. Immune cell infiltration and cytokine secretion analysis reveal a non-inflammatory microenvironment of medulloblastoma. Oncol Lett. 2020;20(6):1-1. doi: 10. 3892/ol.2020.12260.
- 6. Riemondy KA, Venkataraman S, Willard N, Nellan A, Sanford B, Griesinger, AM, Amani V, Mitra S, Hankinson, TC, Handler, MH, et al. Neoplastic and immune single cell transcriptomics define subgroup-specific intra-tumoral heterogeneity of childhood medulloblastoma. Neuro Oncol. 2021;24(2):273-286. doi: 10. 1093/neuonc/noab135.
- 7. Vermeulen JF, Van Hecke W, Adriaansen EJM, Jansen MK, Bouma RG, Villacorta Hidalgo J, Fisch P, Broekhuizen R, Spliet WGM, Kool M, et al. Prognostic relevance of tumor-infiltrating lymphocytes and immune checkpoints in pediatric medulloblastoma. Oncoimmunology. 2018;7(3):e1398877. doi: 10.1080/2162402X.2017.1398877.
- 8. Schakelaar MY, Monnikhof M, Crnko S, Pijnappel EW, Meeldijk J, ten Broeke T, Bovenschen N. Cellular immunotherapy for medulloblastoma. Neuro-Oncol. 2023;25(4):617-627. doi: 10. 1093/neuonc/noac236.
- 9. Khatua S, Cooper LJN, Sandberg DI, Ketonen L, Johnson JM, Rytting ME, Liu DD, Meador H, Trikha P, Nakkula RJ, et al. Phase I study of intraventricular infusions of autologous ex vivo expanded NK cells in children with recurrent medulloblastoma and ependymoma. Neuro Oncol. 2020;22(8):1214-1225. doi: 10. 1093/neuonc/noaa047.
- 10. Mishra A, Maiti R, Mohan P, Gupta P. Antigen loss following CAR-T cell therapy: mechanisms, implications, and potential solutions. Eur J Haematol. 2024;112(2):211-222. doi: 10.1111/ejh.
- 11. Hayday AC. γδ cells: a right time and a right place for a conserved third way of protection. Annu Rev Immunol. 2000;18(1):975-1026. doi: 10.1146/annurev.immunol.18.1.975.
- 12. Willcox BE, Willcox CR. γδ TCR ligands: the quest to solve a 500million-year-old mystery. Nat Immunol. 2019;20(2):121-128. doi: 10.1038/s41590-018-0304-y.
- 13. Chien Y, Meyer C, Bonneville M. γδ T cells: first line of defense and beyond. Annu Rev Immunol. 2014;32(1):121-155. doi: 10.1146/ annurev-immunol-032713-120216.
- 14. Xu Y, Xiang Z, Alnaggar M, Kouakanou L, Li J, He J, Yang J, Hu Y, Chen Y, Lin L, et al. Allogeneic Vγ9Vδ2 T-cell immunotherapy exhibits promising clinical safety and prolongs the survival of patients with late-stage lung or liver cancer. Cell Mol Immunol. 2021;18(2):427-439. doi: 10.1038/s41423-020-0515-7.
- 15. Di Lorenzo B, Simões AE, Caiado F, Tieppo P, Correia DV, Carvalho T, da Silva MG, Déchanet-Merville J, Schumacher TN, Prinz I, et al. Broad cytotoxic targeting of acute myeloid leukemia by polyclonal delta one T cells. Cancer Immunol Res. 2019;7 (4):552-558. doi: 10.1158/2326-6066.CIR-18-0647.

- 16. Lamb LS, Pereboeva L, Youngblood S, Gillespie GY, Nabors LB, Markert JM, Dasgupta A, Langford C, Spencer HT. A combined treatment regimen of mgmt-modified $\gamma\delta\,T$ cells and temozolomide chemotherapy is effective against primary high grade gliomas. Sci Rep. 2021;11(1):21133. doi: 10.1038/s41598-021-00536-8.
- 17. Tosolini M, Pont F, Poupot M, Vergez F, Nicolau-Travers M-L, Vermijlen D, Sarry JE, Dieli F, Fournié J-J. Assessment of tumor-infiltrating TCRVγ9Vδ2 γδ lymphocyte abundance by deconvolution of human cancers microarrays. Oncoimmunology. 2017;6(3):e1284723. doi: 10.1080/2162402X. 2017.1284723.
- 18. Chen B, Khodadoust MS, Liu CL, Newman AM, Alizadeh AA. Profiling tumor infiltrating immune cells with CIBERSORT. Methods Mol Biol. 2018;1711:243-259.
- 19. Song L, Cohen D, Ouyang Z, Cao Y, Hu X, Liu XS. TRUST4: immune repertoire reconstruction from bulk and single-cell RNA-seq data. Nat Methods. 2021;18(6):627-630. doi: 10.1038/ s41592-021-01142-2.
- 20. Pont F, Familiades J, Déjean S, Fruchon S, Cendron D, Poupot M, Poupot R, L'Fagihi-Olive F, Prade N, Ycart B, et al. The gene expression profile of phosphoantigen-specific human γδ T lymphocytes is a blend of $\alpha\beta$ T-cell and nk-cell signatures. Eur J Immunol. 2012;42(1):228-240. doi: 10.1002/eji.201141870.
- 21. Bockmayr M, Mohme M, Klauschen F, Winkler B, Budczies J, Rutkowski S, Schüller U. Subgroup-specific immune and stromal microenvironment in medulloblastoma. Oncoimmunology. 2018;7 (9):e1462430. doi: 10.1080/2162402X.2018.1462430.
- 22. Margol AS, Robison NJ, Gnanachandran J, Hung LT, Kennedy RJ, Vali M, Dhall G, Finlay JL, Erdreich-Epstein A, Krieger MD, et al. Tumor-associated macrophages in SHH subgroup of medulloblastomas. Clin Cancer Res. 2015;21(6):1457-1465. doi: 10.1158/1078-0432.CCR-14-1144.
- 23. Gentles AJ, Newman AM, Liu CL, Bratman SV, Feng W, Kim D, Nair VS, Xu Y, Khuong A, Hoang CD, et al. The prognostic landscape of genes and infiltrating immune cells across human cancers. Nat Med. 2015;21(8):938-945. doi: 10.1038/nm.3909.
- 24. Meraviglia S, Lo Presti E, Tosolini M, La Mendola C, Orlando V, Todaro M, Catalano V, Stassi G, Cicero G, Vieni S, et al. Distinctive features of tumor-infiltrating $\gamma\delta$ T lymphocytes in human colorectal cancer. OncoImmunology. 2017;6(10):e1347742. doi: 10. 1080/2162402X.2017.1347742.
- 25. Zhang XM, Tonnelle C, Lefranc MP, Huck S. T cell receptor y cDNA in human fetal liver and thymus: variable regions of γ chains are restricted to VyI or V9, due to the absence of splicing of the V10 and V11 leader intron. Eur J Immunol. 1994;24(3):571-578. doi: 10.1002/eji.1830240312.
- 26. Aliseychik M, Patrikeev A, Gusev F, Grigorenko A, Andreeva T, Biragyn A, Rogaev E. Dissection of the human T-Cell receptor y gene repertoire in the brain and peripheral blood identifies ageand alzheimer's disease-associated clonotype profiles. Front Immunol. 2020;11:497030. doi: 10.3389/fimmu.2020.00012.
- 27. Papadopoulou M, Dimova T, Shey M, Briel L, Veldtsman H, Khomba N, Africa H, Steyn M, Hanekom WA, Scriba TJ, et al. Fetal public Vγ9Vδ2 T cells expand and gain potent cytotoxic functions early after birth. Proc Natl Acad Sci. 2020;117:18638-18648. doi: 10.1073/pnas.1922595117.
- 28. Ivanov DP, Coyle B, Walker DA, Grabowska AM. In vitro models of medulloblastoma: choosing the right tool for the job. J Biotechnol. 2016;236:10-25. doi: 10.1016/j.jbiotec.2016.07.028.
- 29. Liu D, Song L, Brawley VS, Robison N, Wei J, Gao X, Tian G, Margol A, Ahmed N, Asgharzadeh S, et al. Medulloblastoma expresses CD1d and can be targeted for immunotherapy with NKT cells. Clin Immunol. 2013;149(1):55-64. doi: 10.1016/j.clim. 2013.06.005.
- 30. Harly C, Joyce SP, Domblides C, Bachelet T, Pitard V, Mannat C, Pappalardo A, Couzi L, Netzer S, Massara L, et al. Human γδ T cell sensing of AMPK-dependent metabolic tumor reprogramming through TCR recognition of EphA2. Sci Immunol. 2021;6(61): eaba9010. doi: 10.1126/sciimmunol.aba9010.



- 31. Marlin R, Pappalardo A, Kaminski H, Willcox CR, Pitard V, Netzer S, Khairallah C, Lomenech A-M, Harly C, Bonneville M, et al. Sensing of cell stress by human $\gamma\delta$ tcr-dependent recognition of annexin A2. Proc Natl Acad Sci USA. 2017;114(12):3163-3168. doi: 10.1073/pnas.1621052114.
- 32. Wang X, Mou W, Han W, Xi Y, Chen X, Zhang H, Qin H, Wang H, Ma X, Gui J. Diminished cytolytic activity of $\gamma\delta$ T cells with reduced DNAM-1 expression in neuroblastoma patients. Clin Immunol. 2019;203:63-71. doi: 10.1016/j.clim.2019.04.006.
- 33. Xiao T, Xiao Y, Wang W, Tang YY, Xiao Z, Su M. Targeting EphA2 in cancer. J Hematol & Oncol. 2020;13(1):114. doi: 10.1186/ s13045-020-00944-9.
- 34. Donovan LK, Delaidelli A, Joseph SK, Bielamowicz K, Fousek K, Holgado BL, Manno A, Srikanthan D, Gad AZ, Van Ommeren R, et al. Locoregional delivery of CAR T cells to the cerebrospinal fluid for treatment of metastatic medulloblastoma and ependymoma. Nat Med. 2020;26(5):720-731. doi: 10.1038/ s41591-020-0827-2.
- 35. Weishaupt H, Johansson P, Sundström A, Lubovac-Pilav Z, Olsson B, Nelander S, Swartling FJ. Batch-normalization of cerebellar and medulloblastoma gene expression datasets utilizing empirically defined negative control genes. Bioinformatics. 2019;35(18):3357-3364. doi: 10.1093/bioinformatics/btz066.
- 36. Harly C, Guillaume Y, Nedellec S, Peigné C-M, Mönkkönen H, Mönkkönen J, Li J, Kuball J, Adams EJ, Netzer S, et al. Key implication of CD277/butyrophilin-3 (BTN3A) in cellular stress sensing by a major human $\gamma\delta$ T-cell subset. Blood. 2012;120 (11):2269-2279. doi: 10.1182/blood-2012-05-430470.
- 37. Cano CE, Pasero C, De Gassart A, Kerneur C, Gabriac M, Fullana M, Granarolo E, Hoet R, Scotet E, Rafia C, et al. BTN2A1, an immune checkpoint targeting Vγ9Vδ2 T cell cytotoxicity against malignant cells. Cell Rep. 2021;36(2):109359. doi: 10.1016/j.celrep.2021.109359.

- 38. Abeler-Dörner L, Swamy M, Williams G, Hayday AC, Bas A. Butyrophilins: an emerging family of immune regulators. Trends Immunol. 2012;33(1):34-41. doi: 10.1016/j.it.2011.09.007.
- 39. Tissue expression of BTN3A1 summary the human protein atlas. https://www.proteinatlas.org/ENSG00000026950-BTN3A1 /tissue?utm.
- 40. Uhlén M, et al. Tissue-based map of the human proteome. Science. 2015;25613900. doi: 10.1126/science.1260419. PubMed.
- Dietrich J. Neurotoxicity of cancer therapies. CONTINUUM: lifelong learning in neurology. Continuum: Lifelong Learn Neurol. 2020;26(6):1646. doi: 10.1212/CON.0000000000000943.
- 42. Schmahmann JD. The cerebellum and cognition. Neurosci Lett. 2019;688:62-75. doi: 10.1016/j.neulet.2018.07.005.
- 43. Costa GP, Mensurado S, Silva-Santos B. Therapeutic avenues for γδ T cells in cancer. J Immunother Cancer. 2023;11(11):e007955. doi: 10.1136/jitc-2023-007955.
- 44. Gorsi HS, Malicki DM, Barsan V, Tumblin M, Yeh-Nayre L, Milburn M, Elster JD, Crawford JR. Nivolumab in the treatment of recurrent or refractory pediatric brain tumors: a single institutional experience. J Pediatr Hematol/Oncol. 2019;41(4):e235. doi: 10.1097/MPH.000000000001339.
- 45. Jiang Z-M, Luo W, Wen Q, Liu S-D, Hao P-P, Zhou C-Y, Zhou M-Q, Ma L. Development of genetically engineered iNKT cells expressing TCRs specific for the M. tuberculosis 38-kDa antigen. J Transl Med. 2015;13(1):141. doi: 10.1186/s12967-015-0502-4.
- 46. Rietkötter E, Menck K, Bleckmann A, Farhat K, Schaffrinski M, Schulz M, Hanisch U-K, Binder C, Pukrop T. Zoledronic acid inhibits macrophage/microglia-assisted breast cancer cell invasion. Oncotarget. 2013;4(9):1449-1460. doi: 10.18632/oncotarget.1201.
- 47. Morris EC, Neelapu SS, Giavridis T, Sadelain M. Cytokine release syndrome and associated neurotoxicity in cancer immunotherapy. Nat Rev Immunol. 2022;22(2):85-96. doi: 10.1038/s41577-021-00547-6.